

ORBIT GRAVITY ERROR COVARIANCE

James R Wright^{*}, James Woodburn[†], Son Truong[‡], William Chuba[§]

Abstract

Optimal orbit determination requires a physically connected method to calculate an acceleration error covariance function to drive the filter time-update across each propagation time interval. For gravity modeling errors we derive the orbit covariance function from an acquired covariance matrix on potential function coefficient estimation errors. We employ existing theory, derived from results due to Kaula, Pechenick, and Wright to calculate a double integral in six-dimensions, the gravity orbit covariance function for the filter. Our existing method has been limited to a single potential function, and our algorithm architecture has been limited to a restricted LEO class. Now we have constructed a new method that broadens the algorithm architecture, with applications to EGM96, Lunar Prospector, and GRACE potential functions.

INTRODUCTION

Optimal orbit determination[25] employs a sequential filter-smoother for low altitude orbits. For some cases this requires a physically connected method to calculate an orbit gravity error process noise covariance function $Q_F(t_{k+1}, t_k)$ to drive the filter time-update across each propagation time interval $[t_k, t_{k+1}]$, $t_k \leq t_{k+1}$, $k \in \{0, 1, 2, \dots\}$. We derive the orbit covariance function $Q_F(t_{k+1}, t_k)$ from an acquired covariance matrix P on potential function coefficient estimation errors. We employ existing theory, derived from results due to Kaula[8], Pechenick[18], and Wright[24], to calculate a double iterated integral in six-dimensions, the covariance function $Q_F(t_{k+1}, t_k)$.

The integral evaluation of $Q_F(t_{k+1}, t_k)$ is partitioned as an iterated integral with an inner analytic integral and an outer numerical integral. Inner integrals are calculated and stored once and for all, and outer integrals are evaluated in real-time. This extends prior technique to provide a more general capability using new polynomials to represent the inner integral for $Q_F(t_{k+1}, t_k)$. Previous published methods (e.g., Wright[24]) were limited to a single potential function, and the algorithm architecture was limited to a restricted LEO class. Now we have constructed a new method to calculate $Q_F(t_{k+1}, t_k)$ that broadens the algorithm architecture, with applications to EGM96, Lunar Prospector, and GRACE potential functions.

Filter-Smoother Consistency Test

If $Q_F(t_{k+1}, t_k)$ has adequately captured the covariance matrix P on potential function coefficient errors, and if our acceleration model used for filter-smoother spacecraft trajectory integration is sufficiently accurate, then McReynolds' filter-smoother (FS) consistency test applied to real tracking data becomes a new tool appropriately used to determine whether or not the potential error covariance matrix P is physically realistic. The FS test uncovers a multitude of modeling errors, so its initial failure is not necessarily due to an unrealistic P .

^{*}ODTK Architect, Analytical Graphics, Inc., 220 Valley Creek Blvd, Exton, PA, 19341

[†]Chief Orbital Scientist, Analytical Graphics, Inc.

[‡]Systems Engineer, Analytical Graphics, Inc.

[§]Astrodynamics and Computer Science Senior Engineer, Analytical Graphics, Inc.

Potential Function Extensions

We have applied our new method to acquired potential functions GGM02C, EGM96, and LP100K using associated covariance matrices P^{EGM96} , P^{LP100K} , and P^{GGM02C} . We have used real JASON GPS tracking data for EGM96 and GGM02C, and have used real Lunar Prospector tracking data for LP100K.

THREE PAPER STRUCTURE

This is the first of three interrelated papers. Here we present the mathematics, approximations, theoretical basis, evaluation technique, and procedure used to calculate $Q_F(t_{k+1}, t_k)$. Complete references for the three papers are given in this paper.

The second paper[30] is titled *Sample Orbit Error Covariance Function*. A new sample covariance $Q_S(t_{k+1}, t_k)$, using an ensemble of 1000 numerical orbit integrations with gravity acceleration error perturbations, was constructed to validate $Q_F(t_{k+1}, t_k)$. Graphical comparisons between $Q_S(t_{k+1}, t_k)$ and $Q_F(t_{k+1}, t_k)$ are presented using JASON-EGM96, Lunar Prospector - Lunar Prospector, and JASON-GRACE orbit-potential combinations.

The third paper[31] is titled *Orbit Covariance Inner Integrals with Polynomials*. The third paper presents details polynomial coefficient calculation and storage for the inner covariance integral. The second part of the third paper presents filter-smoother consistency test results on real tracking data for JASON-EGM96, Lunar Prospector - Lunar Prospector, and JASON-GRACE. Appendices present detailed notation for coordinate frames, vectors, and vector components used herein.

COVARIANCE APPROXIMATIONS

The Kaula, Pechenick, and Wright theory used for calculation of the filter covariance function $Q_F(t_{k+1}, t_k)$ invokes approximations (1.) through (5.) that apply to our new method. Approximations (6.) through (12.) are invoked to enable a fast-running filter, sufficiently accurate to capture the essence of the potential function covariance matrix P .

1. The orbit of interest is assumed to be circular with radius r equal to semi-major axis a , or near-circular with $r \approx a$
2. The filter orbit error covariance function $Q_F(t_{k+1}, t_k)$ is derived by averaging gravity model errors over a sphere with radius $r = a$
3. $Q_F(t_{k+1}, t_k)$ is sensitive to orbit initial condition variations in semi-major axis a , but not to variations in other Kepler orbit elements
4. Potential function covariance matrix *variances* are captured by $Q_F(t_{k+1}, t_k)$, but matrix *cross-covariances* are summed out - see Eq. 49
5. Orbit resonance effects are not addressed
6. Two-body mechanics are employed for process-noise covariance propagation
7. The three auto-correlation integrals are approximated as time-constants with selection functions - see Eqs. 73, 74, and 75
8. The zero value for the *intrack* correlation integral is arbitrarily replaced by a small positive number in order to guarantee that $Q_F(t_{k+1}, t_k)$ is positive definite
9. $Q_F(t_{k+1}, t_k)$ is implemented with filter time lag $\Delta t = t_{k+1} - t_k$; default: $\Delta t = 2$ min
10. Our implementation of $Q_F(t_{k+1}, t_k) = I2$, according to Eq. 84, decouples the dependence of $I2$ on $I1$ in the numerical integration of $I2$ as presented in Eqs. 39 through 44

11. A mean-value theorem is invoked to conveniently partition an integrand across $[t_k, t_{k+1}]$ – See Eq. 14
12. For implementation of $Q_F(t_{k+1}, t_k)$, the real non-circular orbit trajectory is approximated by a series of discontinuous circular orbits, each with the correct value of $r = r(t_{k+1}, t_k)$ for some time t in the interval $[t_k, t_{k+1}]$

History

Professor Kaula developed his gravity covariance theory[8] in 1959 to study gravity errors of omission on the Earth’s surface in his geodesy work at UCLA. Gersten[3], Gore, and Hall used Kaula’s theory to calculate orbit perturbations in 1967.

An attempt was made by Wright in 1978 at the General Electric Company (Space Division in King of Prussia) to numerically integrate the double integral defined by Equations 40 through 44 using two-body mechanics in equinoctial¹ orbit elements. Double precision calculation was performed on an IBM 370. Two problems were incurred. First, although the resulting 6×6 matrix was near-symmetric in the top-left corner, it was increasingly less symmetric as one scanned it to the bottom-right corner. The matrix produced was significantly unsymmetric, but the covariance double integral is symmetric by definition. Second, two days of wall-time were required to calculate one matrix for one five-minute filter time-update. These two impediments led directly to the introduction of successful approximations (7.), (8.), (9.) and (10.).

Potential function coefficient uncertainty is formally defined by the covariance matrix P derived in the estimation of the coefficients. Matrix P is usually provided with the coefficient estimates. The uncertainties of the elements in matrix P are unknown, but it would be difficult to show they are realistic beyond two decimals. We use matrix P to derive $Q_F(t_{k+1}, t_k)$. Thus approximations in this section should be considered in terms of the uncertainties of the elements in covariance matrix P , in addition to the utility of these approximations in the construction of a fast-running filter for optimal orbit determination.

STOCHASTIC ORBIT EQUATIONS

Concatenate the 3×1 position and velocity² component arrays $z(t)$ and $\dot{z}(t)$ to form the dynamic orbit representation $Z(t)$:

$$Z = Z(t) = \begin{bmatrix} z(t) \\ \dot{z}(t) \end{bmatrix} = \begin{bmatrix} z_1(t) \\ z_2(t) \\ z_3(t) \\ \dot{z}_1(t) \\ \dot{z}_2(t) \\ \dot{z}_3(t) \end{bmatrix} = \begin{bmatrix} Z_1(t) \\ Z_2(t) \\ Z_3(t) \\ Z_4(t) \\ Z_5(t) \\ Z_6(t) \end{bmatrix} \quad (1)$$

and the constant orbit representation $Z_0 = Z(t_0)$ fixed at t_0 :

$$Z_0 = \begin{bmatrix} z_0 \\ \dot{z}_0 \end{bmatrix} \quad (2)$$

Consider the multi-dimensional linear stochastic differential equation for orbit error $dZ(t)$

$$dZ(t) = F(t) Z(t) dt + G(t) dV(t) \quad (3)$$

where $F(t)$ is a 6×6 deterministic time-varying matrix function, $G(t)$ is a 6×3 time-varying deterministic matrix function, and $V(t)$ is a stochastic time-varying 3×1 matrix functional such that its differential $dV(t)$ is a normal serially-correlated 3×1 matrix stochastic functional. The orbit error $dZ(t)$ is a stochastic functional because the forcing functional $dV(t)$ is stochastic.

¹Herein we calculate $Q_F(t_{k+1}, t_k)$ in position and velocity components.

²See Appendices in the third paper[31] for notational detail on coordinate frames, vectors, and vector components.

A Related Stochastic Differential Equation

The form for Equation 3 appears in many treatises on stochastic differential equations, but never with the condition that $dV(t)$ is a serially-correlated functional. Examples can be found in Bucy and Joseph[1] page 24 Equation 2.6, and Oksendal[16] page 83 Equation 6.1.2. They define $V(t)$ as a Wiener process (Brownian motion or random walk) so that $dV(t)$ is a white noise process. Then using Ito's Lemma[1], $dZ(t)$ has the definite integral $Z(t_{k+1})$ across $[t_k, t_{k+1}]$

$$Z(t_{k+1}) = \Phi(t_{k+1}, t_k) Z(t_k) + \int_{t_k}^{t_{k+1}} \Phi(t_{k+1}, \tau) G(\tau) dV(\tau) \quad (4)$$

where $\Phi(t, t_0)$ is related to $F(t)$ via Equation 24.

A Deterministic Differential Equation

It is useful to note that $dZ(t)$, for the completely deterministic differential equation

$$dZ(t) = F(t) Z(t) dt + G(t) u(t) dt \quad (5)$$

sometimes written

$$\frac{dZ(t)}{dt} = F(t) Z(t) + G(t) u(t) \quad (6)$$

has the definite integral across $[t_k, t_{k+1}]$

$$Z(t_{k+1}) = \Phi(t_{k+1}, t_k) Z(t_k) + \int_{t_k}^{t_{k+1}} \Phi(t_{k+1}, \tau) G(\tau) u(\tau) d\tau \quad (7)$$

Differentiate Equation 7 to get Equation 6, or construct Equation 7 from Equation 6 with the linear theory of variation of parameters.

Equation 6 was adopted *formally* by Kalman as a stochastic differential equation with $u(t)$ re-defined as white noise. See Kalman[6] page 278 Equation 3.1 and page 279, or see Meditch[13] page 144 Equation 4.52. Also, Equation 7 was adopted *formally* as the stochastic integral to Equation 6. See Kalman[6] page 279 Equation 3.5, or see Meditch[13] page 144. The word *formally* was somehow meant to excuse the fact that $dZ(t)/dt$ does not exist if $u(t)$ is white noise.

Our Stochastic Orbit Integral Equation

But our application of Equation 3 to the orbit determination problem requires that $dV(t)$ represent gravity acceleration modeling errors. These errors are serially correlated across every time interval. They are not white. We assume them to be normally distributed, noting support from the Central Limit Theorem. Thus $dV(t)$ is not a white noise process and $V(t)$ is not a Wiener process. Now let $u(\tau)$ denote a normal serially correlated stochastic forcing function and set

$$dV(\tau) = u(\tau) d\tau \quad (8)$$

to transform Equation 7 to the form given by Equation 4, so that $dV(\tau)$ is now a normal serially correlated stochastic forcing function, and $Z(t_{k+1})$ is the definite integral across $[t_k, t_{k+1}]$ with the same structure as both Equations 7 and 4. The same form for the differential equation and its integral equation holds for forcing functions that are deterministic or white.

Matrix Function G

It is useful to recall the rigorous theory of variation of parameters[4][5] (VOP) for this section. Recall Eq.1:

$$Z(t) = \begin{bmatrix} z(t) \\ \dot{z}(t) \end{bmatrix}$$

Run the perturbative derivative (Herrick's grave-derivative[4][5]) through Eq.1:

$$Z'(t) = \begin{bmatrix} 0_{3 \times 1} \\ \dot{z}' \end{bmatrix}_{6 \times 1} \quad (9)$$

where \dot{z}' is the grave³ time derivative of $\dot{z}(t)$, and where:

$$\dot{z}'(t) = 0 \quad (10)$$

because $z(t)$ is referred to an inertial origin. Since:

$$\dot{z}' = \frac{\partial z}{\partial y} \dot{y}' = R_{iu} \dot{y}' \quad (11)$$

where \dot{y}' here represents perturbative gravity acceleration error on the Gaussian frame, then:

$$dZ(t) = \begin{bmatrix} 0_{3 \times 1} \\ R_{iu} \dot{y}' dt \end{bmatrix}_{6 \times 1} \quad (12)$$

and:

$$\int_{t_k}^{t_{k+1}} dZ(t) = \begin{bmatrix} 0_{3 \times 1} \\ \int_{t_k}^{t_{k+1}} R_{iu} \dot{y}' dt \end{bmatrix}_{6 \times 1} \quad (13)$$

Use a particular form of the mean-value theorem to write:

$$\int_{t_k}^{t_{k+1}} R_{iu} \dot{y}' dt = \bar{R}_{iu} \int_{t_k}^{t_{k+1}} \dot{y}' dt \quad (14)$$

Since $\bar{R}_{iu} = \bar{R}_{iu}(t)$ is time dependent, approximate the mean value $\bar{R}_{iu}(t)$ at $t = [t_k + t_{k+1}]/2$:

$$\bar{R}_{iu} = R_{iu} \left(\frac{1}{2} [t_k + t_{k+1}] \right) \quad (15)$$

Define integrals $\delta Z_{k+1,k}$ and $\delta \dot{y}'_{k+1,k}$:

$$\delta Z_{k+1,k} = \int_{t_k}^{t_{k+1}} dZ \quad (16)$$

$$\delta \dot{y}'_{k+1,k} = \int_{t_k}^{t_{k+1}} \dot{y}' dt \quad (17)$$

Then Eq. 13 can be written:

$$\delta Z_{k+1,k} = \begin{bmatrix} 0_{3 \times 1} \\ \bar{R}_{iu} \delta \dot{y}'_{k+1,k} \end{bmatrix}_{6 \times 1} \quad (18)$$

where $\delta \dot{y}'_{k+1,k}$ is the accumulated gravity acceleration error, in Gaussian components, across $[t_k, t_{k+1}]$. Since:

$$\begin{bmatrix} 0_{3 \times 1} \\ \bar{R}_{iu} \delta \dot{y}'_{k+1,k} \end{bmatrix}_{6 \times 1} = \begin{bmatrix} 0_{3 \times 3} \\ \bar{R}_{iu} \end{bmatrix}_{6 \times 3} [\delta \dot{y}']_{3 \times 1} \quad (19)$$

then Eq. 18 can be written with the structure:

$$\delta Z_{k+1,k} = \begin{bmatrix} 0_{3 \times 3} \\ \bar{R}_{iu} \end{bmatrix}_{6 \times 3} [\delta \dot{y}']_{3 \times 1} \quad (20)$$

³See Herrick Vol. 1[4] Section 9H and Vol. 2[5] Chapter 16 for definition of grave (pronounced gräv) derivatives – these are partial derivatives with respect to time. Note that $\dot{z}(t)$ is not referred to an inertial origin, so its grave derivative is non-zero.

Associate the 3×1 matrix $\delta y'$ with accumulated (integrated) gravity acceleration error. Calculate:

$$\bar{R}_{iu} = \bar{R}_{ui}^T \quad (21)$$

after evaluation of \bar{R}_{ui} . Define the 6×3 matrix G with:

$$G = \begin{bmatrix} 0_{3 \times 3} \\ \bar{R}_{iu} \end{bmatrix} \quad (22)$$

Then Eq. 20 becomes:

$$\delta Z_{k+1,k} = G \delta y' \quad (23)$$

Eqs. 23 and 22 are the results required for gravity error process noise. See the integral Eq. 7 for use of matrix G .

Matrix Function F

This section relates matrix function $F(t, t_0)$ to the transition matrix function $\Phi(t, t_0)$. We have no need to calculate $F(t, t_0)$, but its existence is implied by use of $\Phi(t, t_0)$. From Meditch[13] Eq. 2.20:

$$\frac{\partial \Phi(t, t_0)}{\partial t} = F(t, t_0) \Phi(t, t_0) \quad (24)$$

derive:

$$F(t, t_0) = \left[\frac{\partial \Phi(t, t_0)}{\partial t} \right] [\Phi(t, t_0)]^{-1} \quad (25)$$

Lagranges' expressions for propagation of position and velocity component matrices $z(t)$ and $\dot{z}(t)$ are presented by Herrick:

$$z(t) = f(t, t_0) z(t_0) + g(t, t_0) \dot{z}(t_0) \quad (26)$$

$$\dot{z}(t) = \dot{f}(t, t_0) z(t_0) + \dot{g}(t, t_0) \dot{z}(t_0) \quad (27)$$

where $z(t)$ and $\dot{z}(t)$ are 3×1 matrices and $f(t, t_0)$, $g(t, t_0)$, $\dot{f}(t, t_0)$ and $\dot{g}(t, t_0)$ are scalar functions. Eqs. 26 and 27 can be combined with the convenient, but unconventional, matrix structure:

$$\begin{bmatrix} z(t) \\ \dot{z}(t) \end{bmatrix}_{6 \times 1} = \begin{bmatrix} f(t, t_0) & g(t, t_0) \\ \dot{f}(t, t_0) & \dot{g}(t, t_0) \end{bmatrix}_{2 \times 2} \begin{bmatrix} z(t_0) \\ \dot{z}(t_0) \end{bmatrix}_{6 \times 1} \quad (28)$$

Thus:

$$\Phi(t, t_0) = \begin{bmatrix} f(t, t_0) & g(t, t_0) \\ \dot{f}(t, t_0) & \dot{g}(t, t_0) \end{bmatrix}_{2 \times 2} \quad (29)$$

The determinant $|\Phi(t, t_0)|$ of $\Phi(t, t_0)$ is unity:

$$|\Phi(t, t_0)| = 1 \quad (30)$$

Eq. 30 implies global existence of the inverse matrix $[\Phi(t, t_0)]^{-1}$, and this means that $F(t, t_0)$ can always be derived from $\Phi(t, t_0)$. Initial conditions (e.g., for $t = t_0$):

$$f(t, t) = g(t, t) = 1 \quad (31)$$

$$\dot{f}(t, t) = \dot{g}(t, t) = 0 \quad (32)$$

provide:

$$\Phi(t, t) = \Phi(t_0, t_0) = I_{2 \times 2} \quad (33)$$

Differentiate Eq. 29 to get:

$$\frac{\partial \Phi(t, t_0)}{\partial t} = \begin{bmatrix} \dot{f}(t, t_0) & \dot{g}(t, t_0) \\ \ddot{f}(t, t_0) & \ddot{g}(t, t_0) \end{bmatrix} \quad (34)$$

Invert Eq. 29 to get:

$$[\Phi(t, t_0)]^{-1} = \begin{bmatrix} \dot{g}(t, t_0) & -g(t, t_0) \\ -\dot{f}(t, t_0) & f(t, t_0) \end{bmatrix} \quad (35)$$

Use Eq. 25 to find $F(t, t_0)$:

$$F(t, t_0) = \begin{bmatrix} \dot{f}(t, t_0) & \dot{g}(t, t_0) \\ \ddot{f}(t, t_0) & \ddot{g}(t, t_0) \end{bmatrix} \begin{bmatrix} \dot{g}(t, t_0) & -g(t, t_0) \\ -\dot{f}(t, t_0) & f(t, t_0) \end{bmatrix} \quad (36)$$

ORBIT ERROR COVARIANCE BASIS

For each fixed point P_0 on a sphere of radius $r > a_e$, Eqs. 52 through 59 provide a geopotential covariance function $R(\psi)$, derived by averaging the product of acceleration error δg_0 at P_0 with every other acceleration error δg (point P) on the sphere. Consider now the intersection of this sphere with a plane that contains the origin of the sphere. This intersection is a circle with fixed radius r . Refer to this circle as a reference circular spacecraft orbit with semi-major axis $a = r$, eccentricity $e = 0$, spacecraft speed $\dot{s} = \sqrt{\mu/a}$, and two plane orientation parameters; e.g., inclination i and node Ω . Consider a sequence of P_0 points, call them P_k , $k \in \{0, 1, 2, \dots\}$, where each point lies on the circular orbit, is associated with a time t_k , and has a covariance matrix function $R^k(\psi)$ at t_k . Our task in this section is to integrate the 3×3 gravity acceleration error covariance matrices $R^k(\psi)$ with time so as to form 6×6 orbit error covariance matrices $Q_F(t_{k+1}, t_k) = P_{k+1|k}^{\int \int}$, and to accumulate these into a running sequential sum of orbit error covariance matrices $P_{k+1|k}$.

The linear integral error model, particularized to the gravity acceleration error 3×1 matrix δg and the orbit error 6×1 matrix δZ , is given by:

$$\delta Z(t_{k+1}) = \Phi(t_{k+1}, t_k) \delta Z(t_k) + \int_{t_k}^{t_{k+1}} \Phi(t_{k+1}, \tau) G(\tau) \delta g(\tau) d\tau \quad (37)$$

$$k \in \{0, 1, 2, \dots\}$$

where matrix $\Phi(t_{k+1}, \tau)$ is a 6×6 orbit error transition matrix, and matrix $G(\tau)$ is the 6×3 matrix defined by Eq. 22. The matrix product $\Phi(t_{k+1}, \tau) G(\tau) \delta g(\tau)$ transforms acceleration errors $\delta g(\tau)$ at time τ to position and velocity errors at time t_{k+1} . If $t_{k+1} = t_k$, there is no contribution to $\delta Z(t_{k+1})$ from any $\delta g(\tau)$; i.e., it takes time to move acceleration errors to orbit errors. Each gravity acceleration error $\delta g(\tau)$ is random, therefore each orbit error $\delta Z(t_{k+1})$ is also random. The orbit error covariance filter time-update matrix, using the expectation operator $E\{\cdot\}$, is defined by:

$$P_{k+1|k} = E \left\{ \delta Z(t_{k+1}) \delta Z(t_{k+1})^T \right\} \quad (38)$$

Insert Eq. 37 into Eq. 38 to get:

$$P_{k+1|k} = \Phi(t_{k+1}, t_k) P_{k|k} \Phi(t_{k+1}, t_k)^T + P_{k+1,k}^{\int \int} \quad (39)$$

where:

$$P_{k+1,k}^{\int \int} = I_{k+1,k}^C + I_{k+1,k}^L + I_{k+1,k}^R \quad (40)$$

$$I_{k+1,k}^C = \int \int_{t_k}^{t_{k+1}} H(t_{k+1}, \tau) E \{ \delta g(\tau) \delta g^T(t) \} H^T(t_{k+1}, t) d\tau dt \quad (41)$$

$$I_{k+1,k}^L = \Phi(t_{k+1}, t_k) \int_{t_k}^{t_{k+1}} E \{ \delta Z(t_k) \delta g^T(t) \} H^T(t_{k+1}, t) dt \quad (42)$$

$$I_{k+1,k}^R = \int_{t_k}^{t_{k+1}} H(t_{k+1}, \tau) E \{ \delta g(\tau) \delta Z^T(t_k) \} d\tau \Phi^T(t_{k+1}, t_k) \quad (43)$$

$$H(t_{k+1}, \eta) = \Phi(t_{k+1}, \eta) G(\eta) \quad (44)$$

If a measurement is processed at time t_k by the sequential filter, then Eq. 37 should be written:

$$\delta Z(t_{k+1}|t_k) = \Phi(t_{k+1}, t_k) \delta Z(t_k|t_k) + \int_{t_k}^{t_{k+1}} \Phi(t_{k+1}, \tau) G(\tau) \delta g(\tau) d\tau \quad (45)$$

$$k \in \{0, 1, 2, \dots\}$$

to explicitly indicate the use of new information at time t_k . With Kalman notation $Q_F(t_{k+1}, t_k)$

$$Q_F(t_{k+1}, t_k) = P_{k+1,k}^{\int \int} \quad (46)$$

ACCELERATION ERROR AUTO-COVARIANCE FUNCTION

A solution to LaPlace's equation in spherical coordinates has been given by many authors; e.g., Kaula[7]:

$$U = \frac{\mu}{r} \sum_{n=0}^{\infty} \left(\frac{a_e}{r} \right)^n \sum_{m=0}^n P_{nm}(\sin \varphi) [C_{nm} \cos m\lambda + S_{nm} \sin m\lambda] \quad (47)$$

where $P_{n0}(\sin \varphi) = P_n(\sin \varphi)$ are Legendre polynomials, $P_{nm}(\sin \varphi)$ are associated Legendre functions, a_e is the equatorial radius of the reference central-body oblate ellipsoid, μ is the two-body gravitational constant with units distance-cubed per time-squared, and C_{nm} and S_{nm} are constants (integrals over mass dm) of degree n and order m . In practice, n is truncated at some positive integer N ; i.e., $n \leq N$. Examples: for LEO $N = 70$, and for GEO $N = 6$.

Degree Variances

Let \bar{C}_{nm} and \bar{S}_{nm} denote fully normalized geopotential coefficients of degree n and order m . Gravity acceleration errors of omission are incurred when any truncation of Eq. 47 is used. William Kaula defined[8] the degree n variance $\sigma_T^2(n)$, for each degree of truncation of Eq. 47, for his work in geodesy:

$$\sigma_T^2(n) = \left[\frac{\mu^2 (n-1)^2}{a_e^4} \right] \sum_{m=0}^n (\bar{C}_{nm}^2 + \bar{S}_{nm}^2) \quad (48)$$

A similar function was defined by Wright[24] to account for gravity acceleration errors of commission:

$$\sigma_C^2(n) = \left[\frac{\mu^2 (n-1)^2}{a_e^4} \right] \sum_{m=0}^n \left(E \{ (\delta \bar{C}_{nm})^2 \} + E \{ (\delta \bar{S}_{nm})^2 \} \right) \quad (49)$$

where $\delta \bar{C}_{nm}$ and $\delta \bar{S}_{nm}$ are estimation errors for estimates of \bar{C}_{nm} and \bar{S}_{nm} . Eq. 49 sums out the effects of cross-correlations in the potential function covariance matrix. If cross-correlations exist in degree variances of commission, they are not accounted for by $\sigma_C^2(n)$. Combine these functions to define:

$$\sigma_n^2 = \begin{cases} \sigma_T^2(n), & n > N \\ \sigma_C^2(n), & n \leq N \end{cases} \quad (50)$$

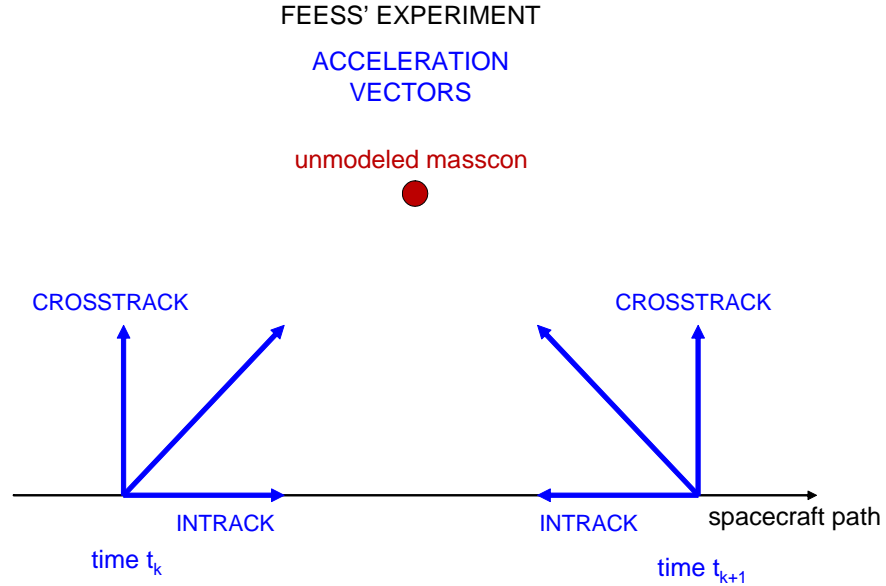


Figure 1: Unmodeled Masscon

Feess' Gedankenexperiment

Figure 1 presents a flat-earth diagram due to Bill Feess[2]. Imagine a perfect geopotential function except for a single unmodeled masscon. So at all times there are radial, intrack, and crosstrack acceleration components, according to Newton's laws, that do not get modeled. Feess' diagram illustrates two of the three acceleration components, intrack and crosstrack, at two times t_k and t_{k+1} . Symmetry of t_k and t_{k+1} with respect to time of closest approach was selected. Notice that the crosstrack acceleration components are "additive" but the intrack acceleration components "subtract out – annihilate themselves". These properties hold for all times while the spacecraft passes the unmodeled masscon because there is approximate acceleration symmetry at times before and after the time of closest approach. The gravity error acceleration equations 52 through 58 quantify the properties illustrated here with Feess' Gedankenexperiment.

Gravity Auto-Covariance

Kaula derived gravity acceleration error auto-covariance functions on a sphere with constant radius r , where the sphere encloses the Earth's surface. Kaula did not publish his derivation. Refer to Fig. 2 for illustration of the orbit sphere with radius r , and the variable central angle ψ . Let P_0 denote a fixed point on the sphere, centered in a surface circle whose radial arc-length ψr subtends angle ψ , and let P denote any point on the surface circle. Thus ψ is the central angle between P_0 and each P . Denote a 3×1 gravity acceleration error matrix δg in Radial, Intrack, and Crosstrack (RIC) components on the Gaussian frame with:

$$\delta g = \begin{bmatrix} \delta g_R \\ \delta g_I \\ \delta g_C \end{bmatrix} \quad (51)$$

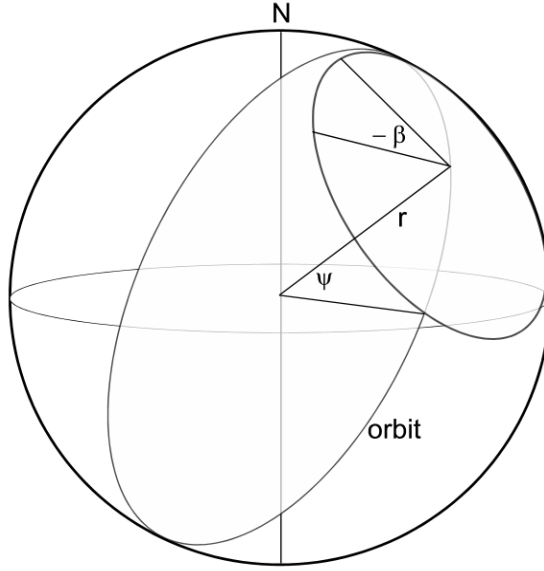


Figure 2: Gravity Error Covariance on Orbit Sphere

Associate point P_0 on the spherical surface with a 3×1 gravity acceleration error matrix δg_0 , and associate each point P on the surface circle with a 3×1 gravity error matrix δg . Assume δg and δg_0 to be unbiased and normally distributed. Kaula developed three RIC scalar auto-covariance component functions of central angle ψ by averaging $E \{ \delta g(P_0) \delta g^T(P) \}$ along the surface circle with one integration, and by averaging $E \{ \delta g(P_0) \delta g^T(P) \}$ over each point P_0 on the spherical surface with two integrations in spherical coordinates. Thus for a fixed radius r , Kaula developed three scalar functions $\sigma_{RR}^2(\psi)$, $\sigma_{II}^2(\psi)$, and $\sigma_{CC}^2(\psi)$ of central angle ψ :

$$\sigma_{RR}^2(\psi) = \sum_n \left[\frac{n+1}{n-1} \right]^2 \left[\frac{a_e}{r} \right]^{2n+4} P_{n0}(\cos \psi) \sigma_n^2 \quad (52)$$

$$\sigma_{II}^2(\psi) = \frac{1}{2} \sum_n \left[\frac{n(n+1)}{(n-1)^2} \right] \left[\frac{a_e}{r} \right]^{2n+4} \left[P_{n0}(\cos \psi) - \frac{P_{n2}(\cos \psi)}{n(n+1)} \right] \sigma_n^2 \quad (53)$$

$$\sigma_{CC}^2(\psi) = \frac{1}{2} \sum_n \left[\frac{n(n+1)}{(n-1)^2} \right] \left[\frac{a_e}{r} \right]^{2n+4} \left[P_{(n-1)0}(\cos \psi) + \frac{P_{(n-1)2}(\cos \psi)}{n(n+1)} \right] \sigma_n^2 \quad (54)$$

This result was derived and extended by Kay Pechenick[18] to include the symmetric off-diagonal covariance expressions:

$$\Gamma_{RI}(\psi) = -\frac{1}{2} \sum_n \left[\frac{n(n+1)^2}{(n-1)^2} \right] \left[\frac{a_e}{r} \right]^{2n+4} \left[P_{(n-1)0}(\cos \psi) + \frac{P_{(n-1)2}(\cos \psi)}{n(n+1)} \right] (\sin \psi) \sigma_n^2 \quad (55)$$

$$\Gamma_{IR}(\psi) = \Gamma_{RI}(\psi) \quad (56)$$

$$\Gamma_{CR}(\psi) = \Gamma_{RC}(\psi) = 0 \quad (57)$$

$$\Gamma_{CI}(\psi) = \Gamma_{IC}(\psi) = 0 \quad (58)$$

Fig. 3 presents a graphical example for auto-covariance functions defined by Eqs. 52, 53, and 54. These functions in radial, in-track, and cross-track gravity acceleration error components are *symmetric* about the origin. Half-function graphics for $0 \leq \psi \leq 180$ degrees are thus sufficient to capture the orbit domain ($-180 \text{ degrees} \leq \psi \leq 180 \text{ degrees}$).

The complete auto-covariance 3×3 matrix function has the structure:

$$R(\psi) = \begin{bmatrix} \sigma_{RR}^2(\psi) & \Gamma_{RI}(\psi) & \Gamma_{RC}(\psi) \\ \Gamma_{IR}(\psi) & \sigma_{II}^2(\psi) & \Gamma_{IC}(\psi) \\ \Gamma_{CR}(\psi) & \Gamma_{CI}(\psi) & \sigma_{CC}^2(\psi) \end{bmatrix} \quad (59)$$

Note that $\sigma_{RR}^2(\psi)$, $\sigma_{II}^2(\psi)$, and $\sigma_{CC}^2(\psi)$ are even functions of ψ , because they are linear combinations of Legendre Polynomials and Associated Legendre Functions of order 2. That is: $R_{jj}(-\psi) = R_{jj}(\psi)$, $j \in \{1, 2, 3\}$. Note also that $\sigma_{RR}^2(\psi)$, $\sigma_{II}^2(\psi)$, and $\sigma_{CC}^2(\psi)$ are positive and attain their maxima at $\psi = 0$. These properties derive from the definition of a *stationary* auto-covariance function $R_{jj}(\psi)$.

From Angle to Time

Let n denote mean orbit motion, a two-body constant. Let t and τ denote arbitrary times, and set:

$$[t - \tau]n = \psi \quad (60)$$

Then:

$$R(\psi) = R([t - \tau]n) \quad (61)$$

Notice that:

$$R([t - \tau]n) = R([(t + T) - (\tau + T)]n) \quad (62)$$

Auto-covariance $R([t - \tau]n)$ may be translated by any time increment T . It is therefore called *stationary*.

$Q_F(t_{k+1}, t_k)$ EVALUATION TECHNIQUE

Covariance Function $R(0)$

For this calculation, the time t is defined implicitly by $r(t)$. Calculate the components of $R(0)$ with $r = r(t)$ fixed⁴:

$$\sigma_{RR}^2(0) = \sum_n \left[\frac{n+1}{n-1} \right]^2 \left[\frac{a_e}{r} \right]^{2n+4} \sigma_n^2 \quad (63)$$

$$\sigma_{II}^2(0) = \frac{1}{2} \sum_n \left[\frac{n(n+1)}{(n-1)^2} \right] \left[\frac{a_e}{r} \right]^{2n+4} \sigma_n^2 \quad (64)$$

$$\sigma_{CC}^2(0) = \frac{1}{2} \sum_n \left[\frac{n(n+1)}{(n-1)^2} \right] \left[\frac{a_e}{r} \right]^{2n+4} \sigma_n^2 \quad (65)$$

$$\Gamma_{RI}(0) = 0 \quad (66)$$

Construct the diagonal matrix $R(0)$:

$$R(0) = \begin{bmatrix} \sigma_{RR}^2(0) & 0 & 0 \\ 0 & \sigma_{II}^2(0) & 0 \\ 0 & 0 & \sigma_{CC}^2(0) \end{bmatrix} \quad (67)$$

⁴The orbit radius $r(t)$ will be treated as a time variable at each step in the sequential filter.

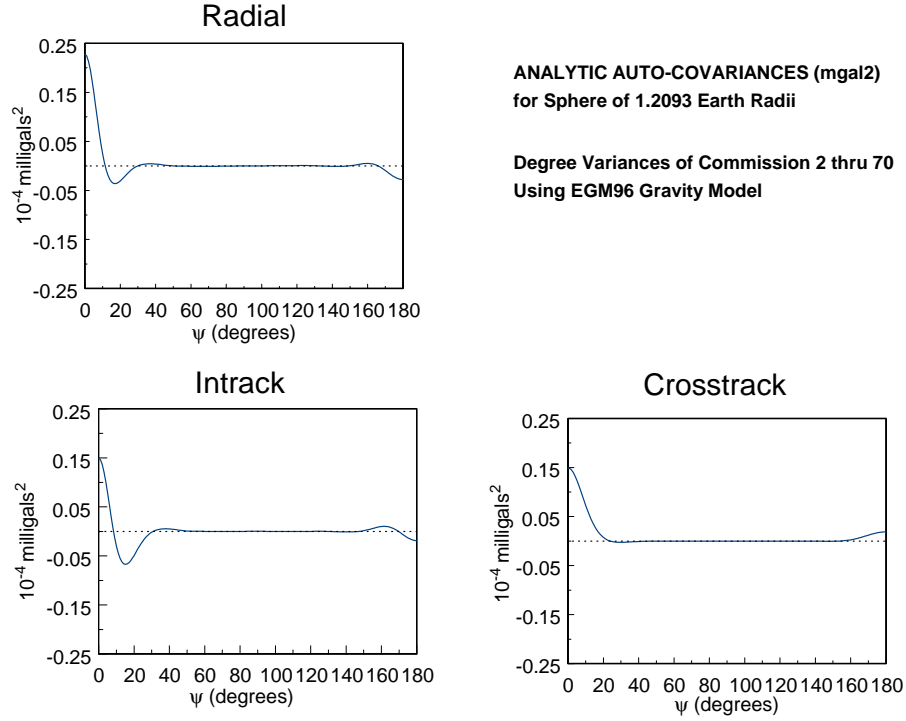


Figure 3: JASON-EGM96 Auto-Covariance Functions

Auto-correlation Function

When $\psi = 0$, the Legendre polynomials are unity, the associated Legendre functions are zero, the instantaneous matrix $R(0)$ is diagonal and has non-zero diagonal elements. This enables the definition of a diagonal 3×3 matrix auto-correlation function:

$$\rho(\psi) = [R(0)]^{-1/2} R(\psi) [R(0)]^{-1/2} \quad (68)$$

and it enables the multiplicative decomposition of $R(\psi)$:

$$R(\psi) = [R(0)]^{1/2} \rho(\psi) [R(0)]^{1/2} \quad (69)$$

Fig. 4 presents a graphical example for the three components of the auto-correlation function defined by Eq. 68. It is important here to notice that the effect of r on $\rho(\psi)$ is divided out, so that significant dynamics due to variations in r are represented in $R(\psi)$ by $[R(0)]^{1/2}$. This is important for implementation.

Auto-correlation Integrals

Denote integrals of functions $\rho_{RR}(\psi)$, $\rho_{II}(\psi)$, and $\rho_{CC}(\psi)$ with $I_{RR}(\psi)$, $I_{II}(\psi)$, and $I_{CC}(\psi)$, and define them with:

$$I_{RR}(\psi) = 2 \int_0^\psi \rho_{RR}(\eta) d\eta \quad (70)$$

$$I_{II}(\psi) = 2 \int_0^\psi \rho_{II}(\eta) d\eta \quad (71)$$

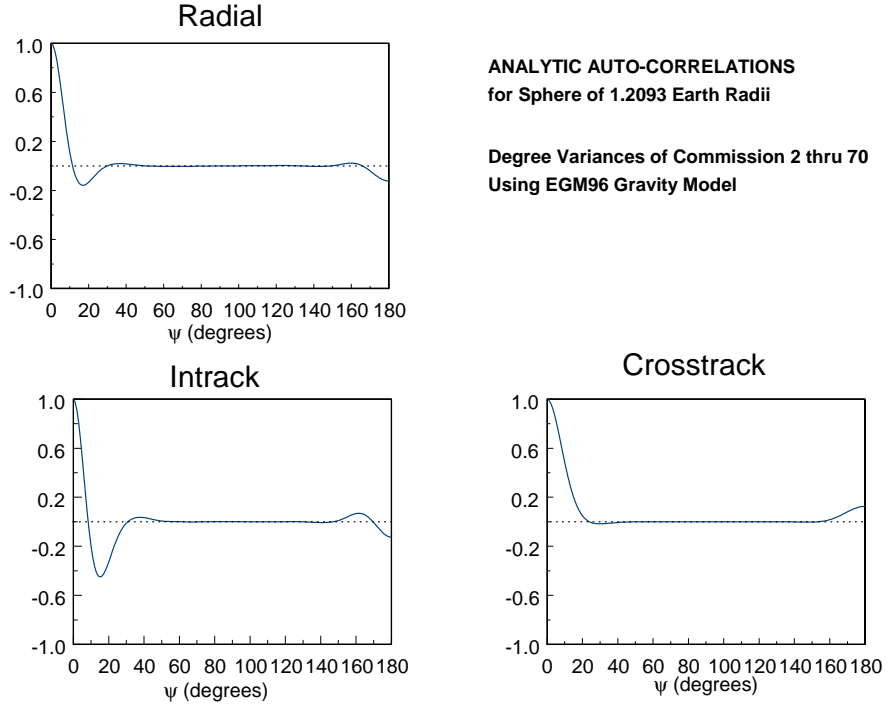


Figure 4: JASON-EGM96 Auto-Correlation Functions

$$I_{CC}(\psi) = 2 \int_0^\psi \rho_{CC}(\eta) d\eta \quad (72)$$

Graph the integral functions $I_{RR}(\psi)$, $I_{II}(\psi)$, and $I_{CC}(\psi)$ in units degrees across the interval $0 \text{ deg} \leq \psi \leq 180 \text{ deg}$. The factor of 2 in each of these equations is to account for symmetry about the origin along the abscissa for $-180 \text{ deg} \leq \psi \leq 180 \text{ deg}$. Each of the integral functions rises from 0 deg at $\psi = 0 \text{ deg}$, and develops an approximate horizontal plateau within $-180 \text{ deg} < \psi < 180 \text{ deg}$. Define a selection function $S(\cdot)$ to select three scalar values \hat{I}_{RR} , \hat{I}_{II} , and \hat{I}_{CC} :

$$\hat{I}_{RR} = S(I_{RR}(\psi)) \quad (73)$$

$$\hat{I}_{II} = S(I_{II}(\psi)) \quad (74)$$

$$\hat{I}_{CC} = S(I_{CC}(\psi)) \quad (75)$$

each to capture its own plateau by ignoring its initial transient. The scalar \hat{I}_{RR} is selected to approximate the function $I_{RR}(\psi)$, the scalar \hat{I}_{II} is selected to approximate the function $I_{II}(\psi)$, and the scalar \hat{I}_{CC} is selected to approximate the function $I_{CC}(\psi)$. The selection of scalars \hat{I}_{RR} , \hat{I}_{II} , and \hat{I}_{CC} is aided by inspection of the graphics for functions $I_{RR}(\psi)$, $I_{II}(\psi)$, and $I_{CC}(\psi)$.

Fig. 5 presents a graphical example for the three JASON-EGM96 auto-correlation integrals defined by Eqs. 70, 71, and 72. The three horizontal integral segments for $(50 \text{ degrees} \leq \psi \leq 150 \text{ degrees})$ are used to define three scalar time-constants to represent the three integrals (Covariance Approximation 7). Notice that the intrack integral is approximately zero for $(50 \text{ degrees} \leq \psi \leq 150 \text{ degrees})$. The scalar constants for JASON at $r = 1.21 \text{ er}$ are: $\hat{I}_{RR} = 9.769 \text{ deg}$, $\hat{I}_{II} = 1.000 \times 10^{-10} \text{ deg}$, and $\hat{I}_{CC} = 20.305 \text{ deg}$.

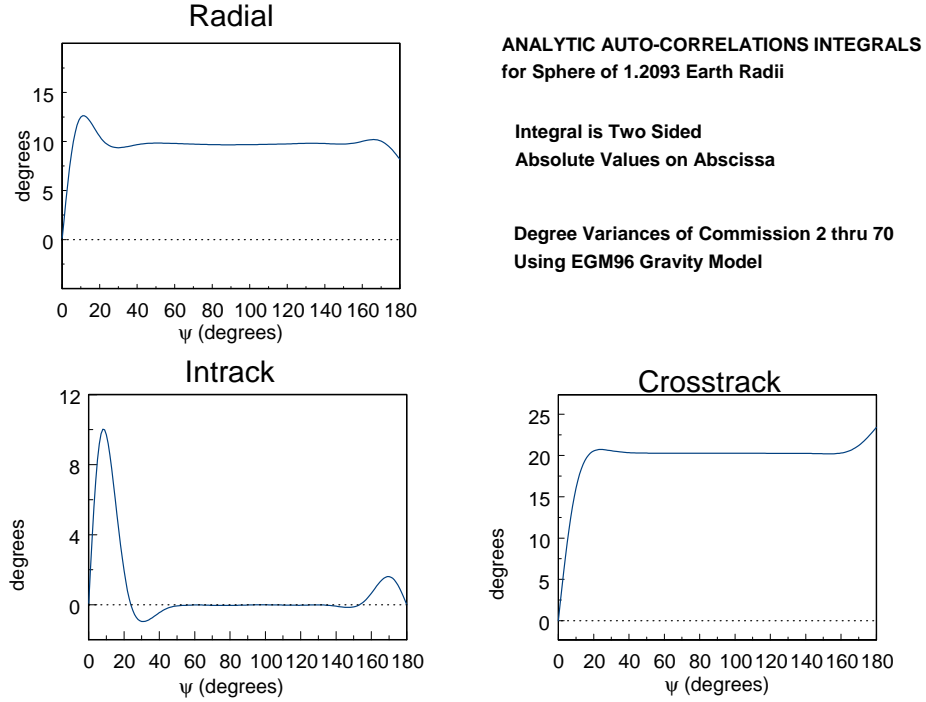


Figure 5: JASON-EGM96 Auto-Correlation Integrals

Convert each integral correlation scalar value \hat{I}_{RR} , \hat{I}_{II} , and \hat{I}_{CC} from units of degrees to units of time \hat{T}_{RR} , \hat{T}_{II} , and \hat{T}_{CC} using the orbit period P mapped onto the 360 degree circle. Select a characteristic value for $r = a$ and calculate mean motion n and orbit period P :

$$n = \left[\frac{\mu}{a^3} \right]^{1/2}$$

$$P = \frac{2\pi}{n}$$

Then our auto-correlation integral values in units time are defined and calculated with:

$$\hat{T}_{RR} = P \left[\frac{\hat{I}_{RR}}{360 \text{ deg}} \right] \quad (76)$$

$$\hat{T}_{II} = P \left[\frac{\hat{I}_{II}}{360 \text{ deg}} \right] \quad (77)$$

$$\hat{T}_{CC} = P \left[\frac{\hat{I}_{CC}}{360 \text{ deg}} \right] \quad (78)$$

Note that \hat{T}_{RR} , \hat{T}_{II} , and \hat{T}_{CC} are functions of r .

Auto-correlation Single Integral Matrix $I1$

Form the diagonal auto-correlation integral 3×3 matrix function $I1$ of r :

$$\mathbf{I1} = \begin{bmatrix} \hat{T}_{RR}(r) & 0 & 0 \\ 0 & \hat{T}_{II}(r) & 0 \\ 0 & 0 & \hat{T}_{CC}(r) \end{bmatrix} \quad (79)$$

and approximate matrix $\mathbf{I1}$ by fitting polynomial functions $\hat{P}_{RR}(r)$, $\hat{P}_{II}(r)$, and $\hat{P}_{CC}(r)$ of r to functions $\hat{T}_{RR}(r)$, $\hat{T}_{II}(r)$, and $\hat{T}_{CC}(r)$ of r :

$$[\mathbf{I1}]_P = \begin{bmatrix} \hat{P}_{RR}(r) & 0 & 0 \\ 0 & \hat{P}_{II}(r) & 0 \\ 0 & 0 & \hat{P}_{CC}(r) \end{bmatrix} \quad (80)$$

The filter process-noise covariance function $\mathbf{I2}$ is a double integral over time. Matrix $\mathbf{I1}$ captures the inner integral with units time.

Time Variation in r

Eqs. 59 and 67 are defined for a fixed value of $r = a$, the radius of an orbit sphere, and the semi-major axis of a circular orbit. In our implementation a new value of $Q_F(t_{k+1}, t_k)$ is calculated on a time grid with granularity $\Delta t = t_{k+1} - t_k > 0$, with default $\Delta t = 2$ minutes. And each new value of $Q_F(t_{k+1}, t_k)$ is associated with a new value of $r = a$. For calculation of $Q_F(t_{k+1}, t_k)$, we think of the real non-circular orbit trajectory as being approximated by a series of discontinuous circular orbits, each with the correct value of $r = r(t_{k+1}, t_k)$ for some time t in the interval $[t_k, t_{k+1}]$. This approximation generates the composite function $R(\psi) = R(\psi(t, r(t)))$. With the partition defined by Eq. 69

$$R(\psi) = [R(0)]^{1/2} \rho(\psi) [R(0)]^{1/2}$$

the variation in $R(\psi(t, r(t)))$ due to the variation in $r(t)$ is captured most significantly by $R(0)$. Thus:

$$R(0) \implies \tilde{R}(0, t)$$

Double Integral Matrix $\mathbf{I2}$

Let t_k and $t_{k+1} > t_k$ be sequential time-tags for filter measurement processing with $t \in [t_k, t_{k+1}]$. Define the 6×3 matrix $H(t_{k+1}, t)$:

$$H(t_{k+1}, t) = \Phi(t_{k+1}, t) G(t) \quad (81)$$

where $\Phi(t_{k+1}, t)$ is the time-varying 6×6 linear transition matrix for ECI position and velocity components from variable time t to fixed time $t_{k+1} > t$, and $G(t)$ is the time-varying 6×3 VOP matrix defined by Eq. 22. Invoke covariance approximations defined above to write:

$$\mathbf{I2} = \int_{t_k}^{t_{k+1}} [H(t_{k+1}, t)] [\tilde{R}(0, t)] [\mathbf{I1}] [H(t_{k+1}, t)]^T dt \quad (82)$$

where:

$$\mathbf{I1} = \int_{-P/2}^{P/2} \rho(\eta) d\eta \quad (83)$$

Eq. 82 presents the orbit error covariance function 6×6 matrix $\mathbf{I2}$ in inertial position and velocity components as an iterated Riemann double integral:

$$\mathbf{I2} = \int_{t_k}^{t_{k+1}} [H(t_{k+1}, t)] [R(0, t)] \left[\int_{-P/2}^{P/2} \rho(\eta) d\eta \right] [H(t_{k+1}, t)]^T dt \quad (84)$$

with the diagonal 3×3 matrix auto-correlation function $\rho(t)$ embedded. We evaluate Eq. 82 with the following time partition and constant time granularity Δ :

$$\begin{bmatrix} t_k = \tau_0 \\ \tau_1 = \tau_0 + \Delta \\ \tau_2 = \tau_1 + \Delta \\ \vdots \\ \tau_{n-1} = \tau_{n-2} + \Delta \\ \tau_n = \tau_{n-1} + \Delta \\ t_{k+1} = \tau_n \end{bmatrix} \quad (85)$$

Define the center time of interval $[\tau_j, \tau_{j+1}]$ with $(\tau_j + \tau_{j+1})/2 = \tau_j + \Delta/2$, $j \in \{0, 1, 2, \dots, n-1\}$. Then Eq. 82 becomes:

$$\mathbf{I2} = \Delta \sum_{j=0}^{n-1} K(\tau_n, \tau_j + \Delta/2) \quad (86)$$

Notice that the transition matrix $\Phi(\tau_n, \tau_j + \Delta/2)$ moves $[G(\tau_j + \Delta/2)][R(0, \tau_j + \Delta/2)][\mathbf{I1}][G(\tau_j + \Delta/2)]^T$ from $(\tau_j + \Delta/2)$ forward to τ_n . This outer integral $\mathbf{I2}$ has other names

$$\mathbf{I2} = Q_F(t_{k+1}, t_k) = P_{k,k+1}^{\int \int} \quad (87)$$

DEVELOPMENT SUMMARY FOR $Q_F(t_{k+1}, t_k)$

Given coefficient values C_{nm} and S_{nm} ($n \in \{0, 1, 2, \dots, N\}$ and $m \in \{0, 1, 2, \dots, n\}$, $m \leq n$) associated with a particular potential function, and given its covariance matrix P for estimation errors δC_{nm} and δS_{nm} , the development of a time-varying orbit covariance function $Q_F(t_{k+1}, t_k)$ is now presented to capture orbit error covariance from the potential function covariance matrix P .

Initial Activities

1. Select a particular gravity potential function and acquire its C_{nm} and S_{nm} values and associated error covariance matrix P , where n denotes degree and m denotes order
2. Identify the positive integer $N = n_{MAX} = m_{MAX}$ for the maximum degree and order provided for the acquired geopotential function (for EGM 96, $N = 70$) and its covariance matrix P

Repeated A Priori Calculations

1. Choose a value for $r = a$, the constant orbit radial distance and semi-major axis for an ideal circular orbit
2. Calculate, tabulate, and store the degree variance values $\sigma_T^2(n)$, $\sigma_C^2(n)$, and σ_n^2 according to Eqs. 48, 49, and 50 for $n \in \{2, 3, \dots, N\}$
3. Graph the covariance functions $\sigma_{RR}^2(\psi)$, $\sigma_{II}^2(\psi)$, and $\sigma_{CC}^2(\psi)$ according to Eqs. 52, 53, and 54, each as a function of ψ for $\psi \in (0, 1, \dots, 179, 180)$ degrees, and note that there is symmetry about the origin along the abscissa
4. Calculate the three numbers $\sigma_{RR}^2(0)$, $\sigma_{II}^2(0)$, and $\sigma_{CC}^2(0)$ according to Eqs. 63, 64, and 65
5. Divide functions $\sigma_{RR}^2(\psi)$, $\sigma_{II}^2(\psi)$, and $\sigma_{CC}^2(\psi)$ by numbers $\sigma_{RR}^2(0)$, $\sigma_{II}^2(0)$, and $\sigma_{CC}^2(0)$ respectively to define auto-correlation functions $\rho_{RR}(\psi) = \sigma_{RR}^2(\psi)/\sigma_{RR}^2(0)$, $\rho_{II}(\psi) = \sigma_{II}^2(\psi)/\sigma_{II}^2(0)$, and $\rho_{CC}(\psi) = \sigma_{CC}^2(\psi)/\sigma_{CC}^2(0)$

6. Graph the auto-correlation functions $\rho_{RR}(\psi)$, $\rho_{II}(\psi)$, and $\rho_{CC}(\psi)$, each as a function of ψ for $\psi \in (0, 1, \dots, 179, 180)$ degrees, and note that there is symmetry about the origin along the abscissa
7. Evaluate and graph the correlation integral functions $I_{RR}(\psi)$, $I_{II}(\psi)$, and $I_{CC}(\psi)$, each as a function of ψ for $\psi \in (0, 1, \dots, 179, 180)$ degrees, according to Eqs. 70, 71, and 72. The factor of 2 in these equations is to account for symmetry about the origin along the abscissa
8. Derive scalar correlation integral values \hat{I}_{RR} , \hat{I}_{II} , and \hat{I}_{CC} from correlation integral functions $I_{RR}(\psi)$, $I_{II}(\psi)$, and $I_{CC}(\psi)$ according to Eqs. 73, 74, and 75
9. Set $\hat{I}_{II} = \epsilon$, where $\epsilon > 0$. From the theory $\hat{I}_{II} \approx 0$, but we replace the zero with $\epsilon > 0$ so as to guarantee a positive definite covariance matrix function
10. Convert each auto-correlation scalar integral value \hat{I}_{RR} , \hat{I}_{II} , and \hat{I}_{CC} from units of degrees to units of time to get \hat{T}_{RR} , \hat{T}_{II} , and \hat{T}_{CC} according to Eqs. 76, 77, and 78

Calculate Polynomial Coefficients

Given repeated calculations of \hat{T}_{RR} , \hat{T}_{II} , and \hat{T}_{CC} with distinct values for $r = a$, treat $\hat{T}_{RR} = \hat{T}_{RR}(r)$, $\hat{T}_{II} = \hat{T}_{II}(r)$, and $\hat{T}_{CC} = \hat{T}_{CC}(r)$ as functions of r .

1. Graph $\hat{T}_{RR}(r)$, $\hat{T}_{II}(r)$, and $\hat{T}_{CC}(r)$ as functions of r
2. Fit interpolating polynomials $\hat{P}_{RR}(r)$, $\hat{P}_{II}(r)$, and $\hat{P}_{CC}(r)$, or polynomial splines, to $\hat{T}_{RR}(r)$, $\hat{T}_{II}(r)$, and $\hat{T}_{CC}(r)$
3. Store the interpolating polynomials $\hat{P}_{RR}(r)$, $\hat{P}_{II}(r)$, and $\hat{P}_{CC}(r)$, or polynomial splines, once and for all for use in the real-time filter

Real-Time Calculations

For each time-update during real-time execution of the sequential filter

1. Input filter propagation interval time values t_k and $t_{k+1} > t_k$
2. Form the diagonal auto-correlation integral 3×3 matrix constant $\mathbf{I1}$ according to Eq. 79 using stored interpolation polynomials $\hat{P}_{RR}(r)$, $\hat{P}_{II}(r)$, and $\hat{P}_{CC}(r)$
3. Calculate the linear orbit two-body transition 6×6 matrix $\Phi(t_{k+1}, t)$
4. Calculate the 6×3 matrix function $G(t_{k+1}, t)$ according to Eq. 22
5. Calculate the 6×3 matrix function $H(t_{k+1}, t)$ according to Eq. 81
6. Implement the 6×6 double integral matrix value $\mathbf{I2}_{k,k+1}$ calculation according to Eq. 86 where

$$\mathbf{I2}_{k,k+1} = Q_F(t_{k+1}, t_k) = P_{k,k+1}^{\int \int} \quad (88)$$

7. Calculate the filter covariance time-update

$$P_{k+1|k} = \Phi_{k,k+1} P_{k|k} \Phi_{k,k+1}^T + Q_F(t_{k+1}, t_k) \quad (89)$$

for each filter covariance propagation over time interval $[t_k, t_{k+1}]$ for $t_{k+1} > t_k$.

References

- [1] Bucy, Richard S., Joseph, Peter D., *Filtering for Stochastic Processes with Applications to Guidance*, Interscience, 1968
- [2] Feess, William, *Private Communications*, 1974
- [3] Gersten, R. H., Gore, R. C., Hall, N. S., *Statistical Properties of Orbit Perturbations Induced by the Earth's Anomalous Gravity*, Journal of Spacecraft, Vol. 4., Sep., 1967, p1150
- [4] Herrick, Samuel, *Astrodynamics*, Vol 1, Van Nostrand, London, 1971
- [5] Herrick, Samuel, *Astrodynamics*, Vol 2, Van Nostrand, London, 1972
- [6] Kalman, R. E., *New Methods in Wiener Filtering Theory*, Proceedings of the First Symposium on Engineering Applications of Random Function Theory and Probability, edited by J. L. Bogdanoff and F. Kozin, John Wiley & Sons, New York, 1963.
- [7] Kaula, William M., *Theory of Satellite Geodesy*, Blaisdell Pub., Mass., 1966
- [8] Kaula, William M., *Statistical and Harmonic Analysis of Gravity*, Journal of Geophysical Research, Vol. 64, Dec. 1959, pp. 2411, 2412, 2418.
- [9] Lass, Harry, *Vector and Tensor Analysis*, McGraw-Hill, New York, 1950
- [10] Stephen McReynolds, *Private Communications*, 1980 to 1998.
- [11] Stephen McReynolds, *Editing Data Using Sequential Smoothing Techniques for Discrete Systems*, AIAA/AAS Astrodynamics Conference, August 20-22, 1984, Seattle, WA.
- [12] Stephen McReynolds, *Filter-Smoother Consistency Test*, Interoffice Memo, Martin Marietta, 21 Feb., 1995
- [13] Meditch, J. S., *Stochastic Optimal Linear Estimation and Control*, McGraw-Hill, New York, 1969.
- [14] Meditch, J. S., *Personal Communications*, 1974.
- [15] Anderson, Brian D. O., Moore, John B., *Optimal Filtering*, Prentice-Hall, New Jersey, 1979.
- [16] Oksendal, Bernt, *Stochastic Differential Equations*, Springer, 6th edition 2003
- [17] Papoulis, A., *Probability, Random Variables, and Stochastic Processes*, McGraw-Hill, New York, 1965.
- [18] Pechenick, K. R., *A Derivation of the Gravity Error Covariance Formulas Including the Off-Diagonal Components*, Applied Technology Associates (ATA), GSFC Contract No. NAS5-29417, September 1988
- [19] Rauch, H. E., *Solutions to the Linear Smoothing Problem*, IEEE Trans. Autom. Control, vol. AC-8, p. 371, 1963
- [20] Davenport, Wilbur B., Root, William L., *An Introduction to the Theory of Random Signals and Noise*, McGraw-Hill, New York, 1958.
- [21] Sherman, S., *A Theorem on Convex Sets with Applications*, Ann. Math. Stat., 26, 763-767, 1955.
- [22] Sherman, S., *Non-Mean-Square Error Criteria*, IRE Transactions on Information Theory, Vol. IT-4, 1958.
- [23] Wiberg, D. M., *Theory and Problems of State Space and Linear Systems*, Schaum's Outline Series, McGraw-Hill, New York, 1971.

- [24] Wright, James R., *Sequential Orbit Determination with Auto-Correlated Gravity Modeling Errors*, AIAA, Journal of Guidance and Control, Vol 4, No. 2, May-June 1981, page 304.
- [25] Wright, James R., *Optimal Orbit Determination*, Paper AAS 02-192, AAS/AIAA Space Flight Mechanics Meeting, San Antonio, Texas, 27-30 Jan., 2002.
- [26] Wright, James R., *Real-Time Estimation of Local Atmospheric Density*, Paper AAS 03-164, 13th AAS/AIAA Space Flight Mechanics Meeting, Ponce, Puerto Rico, 9-13 Feb., 2003
- [27] Wright, James R., Woodburn, James, *Simultaneous Real-Time Estimation of Atmospheric Density and Ballistic Coefficient*, Paper AAS 04-175, 14th AAS/AIAA Space Flight Mechanics Conference, Maui, Hawaii, 8-12 Feb., 2004
- [28] Wright, James R., Tanygin, Sergei, *Removal of Arbitrary Discontinuities in Atmospheric Density*, Paper AAS 04-176, 14th AAS/AIAA Space Flight Mechanics Conference, Maui, Hawaii, 8-12 Feb., 2004
- [29] Wright, James R., *Sherman's Theorem*, The Journal of the Astronautical Sciences, The Malcolm D. Shuster Astronautics Symposium, Vol. 54, Nos. 3 and 4, July-December 2006, pages 299-319
- [30] Wright, James R., Woodburn, James, Truong, Son, Chuba, William, *Sample Orbit Covariance Function and Filter-Smoother Consistency Tests*, 18th AAS/AIAA Space Flight Mechanics Meeting, Paper AAS 08-159, Galveston, TX, January 2008
- [31] Wright, James R., Woodburn, James, Truong, Son, Chuba, William, *Orbit Covariance Inner Integrals with Polynomials*, 18th AAS/AIAA Space Flight Mechanics Meeting, Paper AAS 08-161, Galveston, TX, January 2008